GARF: Geometry-Aware Generalized Neural Radiance Field

Yue Shi,[1] **Dingyi Rong,** [1] **Bingbing Ni,** [1] **Chang Chen,** [1] **Wenjun Zhang** [1]

[1] Shanghai Jiao Tong University

shiyue001@sjtu.edu.cn, r892546826@sjtu.edu.cn, nibingbing@sjtu.edu.cn¿, chenchang@sjtu.edu.cn, zhangwenjun@sjtu.edu.cn

Abstract

Neural Radiance Field (NeRF) has revolutionized free viewpoint rendering tasks and achieved impressive results. However, the efficiency and accuracy problems hinder its wide applications. To address these issues, we propose Geometry-Aware Generalized Neural Radiance Field (GARF) with a geometry-aware dynamic sampling (GADS) strategy to perform real-time novel view rendering and unsupervised depth estimation on unseen scenes without per-scene optimization. Distinct from most existing generalized NeRFs, our framework infers the unseen scenes on both pixel-scale and geometry-scale with only a few input images. More specifically, our method learns common attributes of novel-view synthesis by an encoder-decoder structure and a point-level learnable multi-view feature fusion module which helps avoid occlusion. To preserve scene characteristics in the generalized model, we introduce an unsupervised depth estimation module to derive the coarse geometry, narrow down the ray sampling interval to proximity space of the estimated surface and sample in expectation maximum position, constituting Geometry-Aware Dynamic Sampling strategy (GADS). Moreover, we introduce a Multi-level Semantic Consistency loss (MSC) to assist more informative representation learning. Extensive experiments on indoor and outdoor datasets show that comparing with state-of-the-art generalized NeRF methods, GARF reduces samples by more than 25%, while improving rendering quality and 3D geometry estimation.

Introduction

Novel-view synthesis is a vital research topic in computer vision, playing a key role in augmented reality, creative interaction, 3D reconstruction, etc. However, the most popular novel-view synthesis methods represented by NeRF (Mildenhall et al. 2020) are still facing many challenges, especially the efficiency and generalizability of both rendering and geometry estimation. Therefore, designing a geometry-aware generalized neural radiance field is meaningful.

The efficiency of neural radiance field mainly depends on its sampling rule and training strategy. For the sampling process, the original NeRF and many follow-up work (Meng et al. 2021; Yu et al. 2021c; Wang et al. 2021) query points along camera rays in whole volume. A series of methods (Liu et al. 2020; Yu et al. 2021b) combine radiance field with

volumetric representation and prune redundant parts of pre-trained neural radiation field to speed up rendering, taking huge memory during training. More importantly, consumption of time and computing resources in training cannot be ignored. Therefore, a scene-adaptive importance sampling scheme needs to be designed to help speed up training and rendering. It is therefore plausible to make NeRF generalize to unseen scenes, and generate novel-view images based on only a limited number of input views and images. Recent work has explored using feature learning to make neural radiance field generalized, i.e., PixelNeRF (Yu et al. 2021c), which takes spatial image feature aligned to each pixel. But learning of common features unavoidably compromises rendering quality and geometry estimation accuracy. **Hence, a framework for learning commonalities while preserving scene uniqueness is urgently needed.**

To improve accuracy while maintaining generalization, previous attempt is to combine pixel colors with image features before learning, which has been proven useful in MVS-NeRf (Chen et al. 2021) and IBRNet (Wang et al. 2021). Besides, MVSNeRF (Chen et al. 2021) and SRF (Chibane et al. 2021) introduce the block matching inspired by MVS (Yao et al. 2018). However, experiments show that generalized NeRFs (Yu et al. 2021c; Wang et al. 2021; Chibane et al. 2021) perform poorly on the geometry, which prevents them from further improving rendering quality. **Therefore, it is essential to address rendering and geometry estimation tasks in a simultaneous and integrated way, instead of tackling them separately. Besides, using the pixel-level optimization objective way also hinders the NeRF networks from learning more representative features.**

To address these issues, we propose a geometry-aware generalized radiance field (GARF) with a geometry-aware dynamic sampling (GADS) strategy, which is capable of fast recovering the unseen scene in both pixel-level and geometry-level, depending on only a few input images. The model learns common attributes of novel-view synthesis in different scenes to acquire generalization to unseen scenes and keeps specific to each scene based on the prior of its estimated geometry. The proposed framework is shown in Fig. 1, which contains a depth estimation module, a feature extraction and fusion module, a geometry-aware dynamic sampling module and a volumetric rendering module. First, we train a self-supervised depth estimation network to get

depth maps for scenes. Based on the initial depth estimation, we narrow the ray sampling interval down to proximity space of the estimated surface. In the sampling interval, we propose a predict-then-refine strategy to progressively approach the most likely location of surface point. For each sampling point, we derive its feature by fusing corresponding multi-view feature vectors learned by a feature extraction network with a set of learnable weights. Finally, we decode the feature of per point into density and color, which are used for volumetric rendering. In order to make the network learn more comprehensive representation, we introduce a Multi-level Semantic Consistency loss (MSC), which integrates both pixel-level loss and semantic feature matching loss to constrain the global similarity of predicted images and the ground truth with limited computational cost. Extensive experiments on indoor and outdoor datasets show that comparing with existing generalized NeRF methods, GARF reduces sampling points by more than 25%, while improving rendering quality and 3D geometry estimation without per-scene optimization.

Related Work

Novel View Synthesis.　Novel view synthesis is to generate the image of the target view from the inputted images. Historically, synthesizing novel views from a set of reference images is conducted by a weighted blending of reference pixels (Debevec, Taylor, and Malik 1996; Gortler et al. 1996; Levoy and Hanrahan 1996). Blending weights are computed based on ray-space proximity (Levoy and Hanrahan 1996) or approximate proxy geometry (Buehler et al. 2001; Heigl et al. 1999). In recent works, researchers have proposed improved methods for computing proxy geometry (Chaurasia et al. 2013; Hedman et al. 2016), optical flow correction (Casas et al. 2015; Eisemann et al. 2008), and soft blending (Penner and Zhang 2017). While these methods can handle sparser views than other approaches, they are limited by the performance of 3D reconstruction algorithms and have difficulties in low-textured regions or reflective regions. Multi-plane images (MPIs) approaches (Flynn et al. 2019, 2016; Mildenhall et al. 2019) have shown remarkable results on continuous view synthesis, but the large number of inputs and samples results in extensive memory overhead, limits the resolution of their outputs.

NeRF.　Neural radiance field (NeRF) (Mildenhall et al. 2020) revolutionized the novel-view synthesis by introducing implicit function to volumetric rendering, bringing out impressive results in complex scenes. To gain more controllable created content, Niemeyer et. al. (Meng et al. 2021; Niemeyer and Geiger 2021) incorporate a compositional 3D scene representation into the generative model. GNeRF combines Generative Adversarial Networks (GAN) with NeRF for complex scenarios with unknown and even randomly initialized camera poses. While NeRF and its follow-up works have achieved impressive results, they must be optimized for each new scene, requiring a large number of input images and taking days to converge. Though several methods have proposed to train on fewer views or render faster (Yu et al. 2021a,b; Liu et al. 2020; Arandjelovic and

Zisserman 2021), non-generalizability of the models still hinders real-time inference.

Generalized NeRF.　A pioneer generalized NeRF framework is proposed by pixelNeRF (Yu et al. 2021c). By introducing image features, pixelNeRF can be trained across multiple scenes. To improve image quality when generalized to novel scenes, IBRNet (Wang et al. 2021) designs a ray transformer to take advantage of the contextual information on the ray. Similar ray transformer structure is also used by GRF (Trevithick and Yang 2021). GRF learns local features for each pixel in images and integrates an attention mechanism(Trevithick and Yang 2021). Stereo Radiance Fields (SRF) (Chibane et al. 2021) introduces patch matching into neural view synthesis to realize sparse inputs. MVSNeRF (Chen et al. 2021) leverages plane-swept cost volumes to improve the performance of the generalized nerf. However, above generalized methods inherit the sampling strategy of the original NeRF (Mildenhall et al. 2020), which samples in the whole space inefficiently. Besides, generalized learning makes the network tend to learn only the interpolation of images in the pixel scale, without geometry learning. The lack of geometric information leads to constraints on generalization capabilities, inefficient rendering, and blurring of novel-view synthesis, especially when the input views are sparse. DS-NeRF (Deng et al. 2021) proposes a loss to take advantage of depth, exploiting the insight that sparse depth supervision can be used to regularize the learned geometry. But the constraint in (Deng et al. 2021) is sparse and the depth prior limits the prediction. We propose GARF framework and GADS scheme to realize geometry-aware sampling and learning.

Methodology

The original NeRF (Mildenhall et al. 2020) optimizes each scene independently, hindering real-time scene reconstruction and rendering application. Though some generalized NeRF-based methods (Yu et al. 2021c; Wang et al. 2021; Chen et al. 2021) attempt to learn common attributes of novel-view synthesis in varying scenes, they are still far from achieving realistic rendering quality or handling large scene and view-angle changes, since these methods lack a principled way to encode sufficient inherent geometric information among multi-view images. Besides, sampling in an unconstrained high-dimensional space makes these NeRFs computationally expensive, hindering their potential application in portable platform. Focusing on above problems, we design a Geometry-Aware Generalized Neural Radiance Field (GARF) model to realize more efficient and higher-fidelity novel scene rendering and depth estimation based on learnable geometry priors. The overall framework is shown in Fig. 1, which consists of two novel components, i.e., a geometry representation learning module along with position and orientation encodings to achieve both generalization and scene-specific details, as well as a Geometry-Aware Dynamic Sampling Strategy (GADS) to realize more accurate and efficient sampling via coarsely inferred geometry (i.e., depth estimation) guidance. In addition, we propose a Multi-level Semantic Consistency Loss (MSC) to facilitate

learning more informative representation.

Generalized Neural Radiance Field

The goal is to predict color and density at point with coordinate x in 3D space, given $\mathcal{I} = \{I_i, P_i\}_{i=1}^{N}$, a set of N input reference images, with camera parameters. Neural radiance fields were initially proposed in NeRF (Mildenhall et al. 2020) and become popular recently for their geometric superiority in processing multi-view images. The main idea of NeRF is utilizing implicit deep model to fit the distribution of color and density of points, which are parameterized by real-valued coordinates and viewing directions of the considered 3D volume, supervised by images captured from multiple view angles. However, NeRF has no cross-scene generalization capability, due to the large semantic gap between input coordinates and output image pixel values, i.e., no semantic features that can encode geometric commonalities. Therefore, in order to cope with unseen scenes, we design a geometric structure representation learnable NeRF by a deep encoder-decoder framework. Specifically, we extract deep convolution features representing the geometry, shape, texture, etc. of input images by an encoder module and fuse multi-view features for representing each point in the 3D space semantically. Then, this novelly introduced scene representation combined with the original coordinate query eliminates the semantic gap of implicit mapping and enhances generalization via commonality learning. In this sense, our goal is to learn a function f_{GARF} which maps the point x_j, feature $F(x_j)$ and view direction r of the point to color c and opacity σ, described as follows:

$$f_{GARF} : (F(x_j), x_j, r) \mapsto (c, \sigma), \qquad (1)$$

In the following, we will introduce the proposed encoder-decoder structure in detail.

Encoder and Feature Fusion.   In contrast to NeRF, where the inputs are point coordinates without scene-specific information, we condition our prediction on the reference images. Specifically, we first use a U-ResNet to extract the feature $M_i \in \mathcal{R}^{H \times W \times z}$ of the image $I_i \in [0, 1]^{H \times W \times 3}$. The skip connection module of U-ResNet better reveals low-level information of the images while preserving global scene structure, which helps generalize to realistic novel-view images. In addition, to check the consistency among the features M_i, we concatenate the image feature with its mean and variance map. The concatenated feature is fed in a PointNet-like MLP to integrate local and global information and generate multi-view aware features W_n, along with a set of learnable weights ω_n.

Then, we fuse the features of different N views together. Previous feature fusing methods in multi-view synthesis use average weighting or weighting based on the distance between the reference view and target view. Actually, the correlation between each 3D point and the multi-view images is different, which cannot be described by the same weight. SRF (Chibane et al. 2021) proposes using patch matching to set reasonable weights, depending on huge memory. We achieve feature fusion in point-wise, projecting every 3D point into each reference view, extracting the corresponding

local features of each view and fusing them together. We use a set of learnable weights for every point to fuse multi-view features. For a target view, a camera ray can be parameterized as $\mathbf{r}(t) = \mathbf{o} + t\mathbf{d}$, with the ray origin (camera center) $\mathbf{o} \in R^3$ and ray unit direction vector $\mathbf{d}$. Taking point x_j in Fig. 1 as an example, we get its feature by reflecting it to feature maps of N input images along corresponding viewing direction r_i as Eq.(2). Consequently, we get the feature V_j^i from view i as Eq.(3), where $proj(\cdot)$ represents the coordinate obtained by the projection of point x_j onto feature cube W_i along the ray r_i. $\mathbf{x}_j$ is the coordinate of point x_j.

$$\mathbf{r}_i = \mathbf{o}_i + t(\mathbf{x}_j - \mathbf{o}_i). \qquad (2)$$
$$V_j^i = W_i [proj(\mathbf{x}_j, \mathbf{r}_i)] \qquad (3)$$

Because of the occlusion and illumination, different perspectives contribute differently to the same point. Therefore, to realize more accurate and view-dependent results, we utilize a set of learnable parameter w_i to weighting N different views. The fused feature $F(x_j)$ for point x_j is:

$$F(x_j) = \sum_{i=1}^{N} w_i V_j^i. \qquad (4)$$

Decoder and Volumetric Rendering.   We have already introduced how to represent a volumetric radiance field conditioned on deeply learned scene features. Here, we introduce how the decoder maps the feature representation into color and density for every sample point. In contrast to most NeRF models which utilize MLP as the decoding structure, in this work we adopt the transformer structure in (Wang et al. 2021) to perform feature decoding of sample sequences on the viewing ray in a context-aware manner. Namely, spatially nearby samples present correlated characteristics; however, MLP independently processes each 3D point without considering the geometry correlations among adjacent samples. On the contrary, transformer-based structures perform self-attention operations, so that contextual dependencies are well modeled and all samples are inferred in a joint way. Based on this decoder structure, for color, we predict the blending weights for the image colors for variation reduction and improve the visual quality of the synthesized results. After getting the color and density value at continuous 5D location, we use volumetric rendering method (Curless and Levoy 1996; Niemeyer et al. 2020a,b) to calculate the color value for every pixel. More concretely, we first query the colors and densities of M samples on the viewing ray, and then we accumulate colors along the ray $\mathbf{r}$ to derive the pixel color $\hat{C}_r$ value as:

$$\hat{C}_r = \sum_{j=1}^{M} T_j (1 - exp(-\sigma_j \delta_j)) c_j, \qquad (5)$$
$$T_j = exp(-\sum_{k=1}^{j-1} \sigma_k \delta_k), \qquad (6)$$

where samples from 1 to M are sorted according to ascending depth values. c_j and σ_j denote the color and density of the jth sample on the ray, respectively. δ_j is the distance between jth sample and $(j-1)th$ sample. In the following section, we will show our innovation on how to accelerate this sampling process.
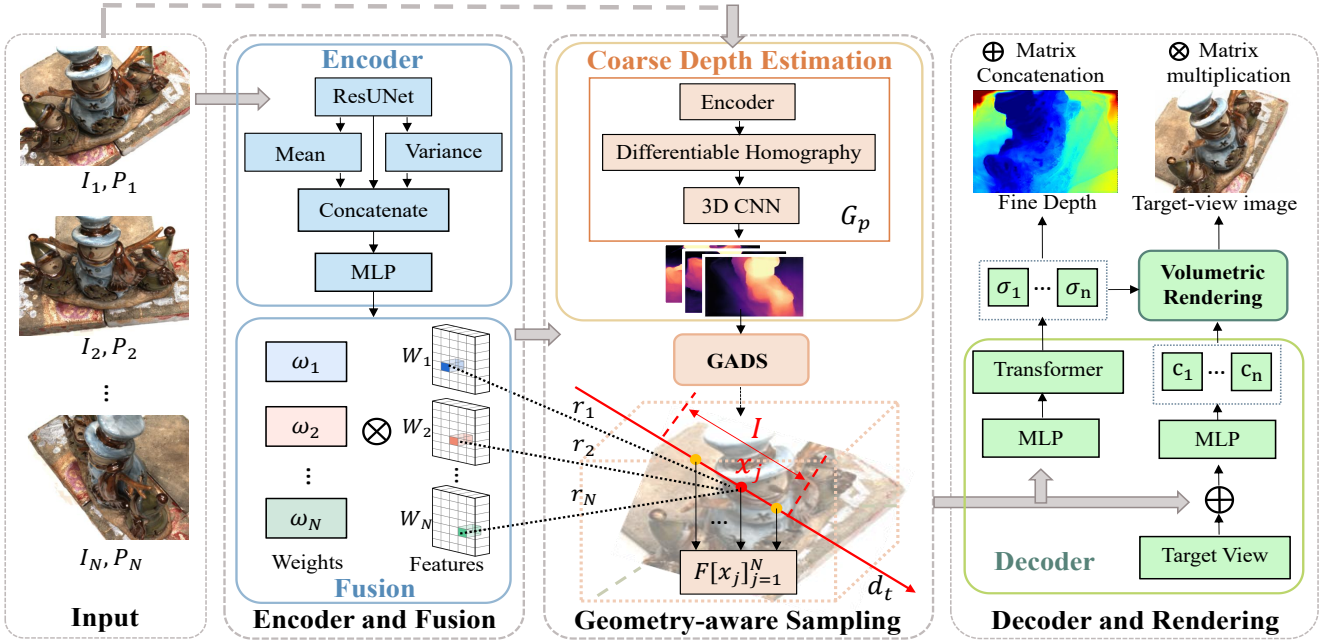
Figure 1: Our framework. The proposed Geometry-Aware Generalized Neural Radiance Field (GARF) consists of three parts. First, deep convolutional features are extracted from input images to form learnable geometry priors of the scene. Second, a dynamic sampling strategy is derived, based on coarsely estimated geometry prior. Finally, a decoder module is designed to predict color and density to render novel-view image along with fine depth map inference in a joint manner.
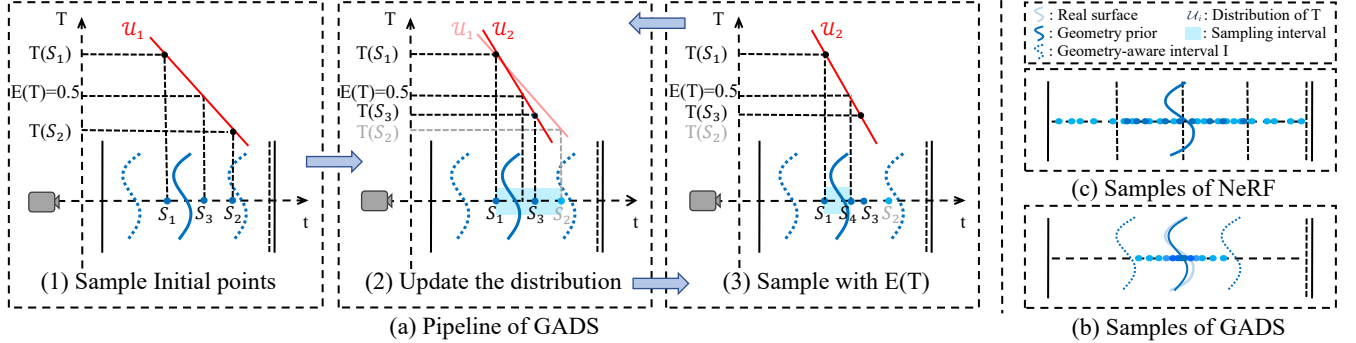

Figure 2: Illustration of the geometry-aware dynamic sampling.

Geometry-Aware Dynamic Sampling

Sampling and integrating along the ray is the most computationally expensive stage in neural rendering. Vanilla sampling strategy in NeRF, which explores the entire 3D volume, not only wastes a lot of computation in empty space but also brings redundant points far away from the real surface, leading to blurry and wrong geometry. To this end, we propose a Geometry-Aware Dynamic Sampling Scheme (GADS) to realize more accurate and efficient sampling. We show the samples of GADS and NeRF in Fig. 2 (b) and (c). The main idea of GADS is two-fold: 1) leveraging the coarse geometry estimated from input images to get a geometry-aware sampling interval, and 2) a dynamic *Predict-then-Refine* sampling strategy to adaptively sample points that are most likely to be close to the geometry surface. Note that GADS realizes both high efficiency and geometry accuracy.

Geometry-aware Sampling Interval. To narrow down the sampling space, we estimate the geometry surface of

the scene and sample in the nearby region. As the coarse depth estimation shown in Fig. 1, we follow MVSNet (Yao et al. 2018) to build a plane-swept cost volume by warping 2D image features from neighboring viewpoints using differentiable homography and then regress depth probability volume using deep 3D CNNs. The depth map is computed by linearly combining per-plane depth values weighted by the probabilities, i.e. the transparency in NeRF. The coarse depth estimation is unsupervised and is optimized by minimizing the distance between predicted depth and the point clouds derived by COLMAP. After rescaling the depth to the GARF space, we exploit it as a geometry prior for sampling. Then, based on the coarse depth d_c, we restrict the sampling operation in an interval I that encloses the space where the surface is most likely to appear, denoted by

$$I = [d_c - \Delta d, d_c + \Delta d]. \tag{7}$$

In this way, we adapt the sampling process to scene geometries. Moreover, because of the adjustable interval Δd, inac-

curate depth estimation has the opportunity to be corrected in the subsequent optimization of the neural radiance field.

Dynamic Sampling Strategy   When the sampling interval is determined, we propose a dynamic sampling strategy (i.e., a new importance sampling scheme), which is shown in Fig. 2 (a). Comparing with stratified sampling in (Mildenhall et al. 2020; Wang et al. 2021; Chen et al. 2021), dynamic sampling realizes accurate geometry-aware sampling by iteratively modifying the target sampling position according to the current position, i.e., in the sense of Markov Chain Monte Carlo (MCMC) (Geyer 1992). Leveraging the idea of MCMC, dynamic sampling progressively approaches the scene surface with just a few samples. To initialize, we randomly sample three points s_0, s_1 and s_2 in the interval, predict their density and derive their accumulated transmittances, as shown in Fig. 2 (a)(1). Supposing that the distribution of the monotonically decreasing T on the ray $\mathbf{r}(t) = \mathbf{o} + t\mathbf{d}$ is linear in a small sampling interval I, we derive the distribution $\mathcal{U}_1$ of T based on the $T(s_1)$ and $T(s_2)$. Then we sample the next point s_3 at the position where the expectation of T is 0.5. The iso-surface with T equal to 0.5 is the implicit surface of NeRF and is usually used to obtain point clouds or meshes from NeRF. In this way, the sample is most likely to be the intersection of the surface and the ray. Then we predict the density of s_3, calculate $T(s_3)$, and use it to update the distribution of the T to $\mathcal{U}_2$ in the sampling interval. According to this rule, the position of the sampling point x_n is decided by t_n which satisfies:

$$t_n = \{t \mid E(T(s_n)) = 0.5, T \sim \mathcal{U}_{n-1}\}. \qquad (8)$$

We repeat this *Predict-then-Refine* operation cyclically until reaching the number of samples we set. To reduce the interference caused by background and depth estimation error, we also take coarse uniform sampling in the interval before dynamic sampling. Note that GADS introduces no extra overhead since the total number of summations in progressive sampling is approximately equal to the number of summations in traditional NeRF with the same sample points.

With the cooperation of geometry-aware sampling interval and dynamic sampling strategy, we find that the points approach the real surface very closely with a limited amount of computation, which means that our model is also capable of performing depth estimation in an unsupervised and generalized way, in addition to the novel view rendering task. In the inference stage, we estimate a fine depth map from neural radiance field by weighting and summing the depth values of the sampled points on marched rays (as is done in (Meng et al. 2021)). The most related work in depth estimation is NerfingMVS (Wei et al. 2021), which is not generalizable. As for generalized NeRF methods (Yu et al. 2021c; Wang et al. 2021), they have no access to accurate depth map, diluting the geometric information during generalization for the pixel-scale optimization goal, as shown in Fig. 4. But in our GARF, we introduce geometry prior for every scene by GADS scheme, which helps GARF learn to infer the geometric layout of the scene.

Optimization Objectives

We train the GARF framework based on the pixel value similarity between the rendered novel view image and its corresponding ground truth. In most NeRF methods, the rendering error is evaluated using only the squared error loss between the rendered and true pixel colors:

$$\mathcal{L}_s = \sum_{r \in \mathcal{R}} \left\| \hat{C}_r - C_r \right\|_2^2, \qquad (9)$$

where $\mathcal{R}$ is the set of rays in each batch. $\mathcal{L}_s$ can only constrain the similarity in pixel-level and does not measure the overall semantic similarity of images. Thus, in order to learn more informative representation, we take the image content and the scene structure into account and propose a Multi-level Semantic Consistency Loss (MSC):

$$\mathcal{L}_{MSC} = \sum_{i=1}^{m} \left\| Encoder(\hat{I}) - Encoder(I) \right\|_2^2, \qquad (10)$$

where m is the number of the encoder output layers of different depths, helping to capture multi-scale semantic information. We take VGG-16 as the encoder $Encoder(\cdot)$ and set m equal to 3 empirically in our experiments. $\hat{I}$ and I are the predicted image and the ground truth image correspondingly. $\mathcal{L}_{MSC}$ makes the network learn semantic-level representation of scenes and take semantic coherence as contextual information to render more realistic novel-view images. In practice, we utilize random samples on the image to participate in the calculation. The Geometry-Aware Dynamic Sampling Scheme (GADS) mentioned above also provides efficiency guarantee for the computing cost of $\mathcal{L}_{MSC}$. Finally, the optimization objective of the GARF network is summarized as:

$$\mathcal{L} = \alpha \mathcal{L}_s + \beta \mathcal{L}_{MSC}, \qquad (11)$$

where α, β are coefficients of the corresponding objectives.

Experiments

Settings

Datasets.   We conduct experiments on DTU MVS Dataset (DTU) and Local Lightfield Fusion Dataset (LLFF), containing both indoor and outdoor scenes. We use camera parameters provided by the two datasets. In our experiment, we down-sample DTU to a resolution of 300×400 for training and evaluation. Images of LLFF are down-sampled to 640×960. For dividing training and test set, and we follow the partition of IBRNet (Wang et al. 2021). There is no intersection between training and test sets, ensuring the validity of generalization tests. For each target view, we randomly select 5 reference views as the input. We keep the sparsity of input views the same as the (Wang et al. 2021).

Evaluation Metrics.   We evaluate image quality by PSNR, SSIM, and LPIPS (Zhang et al. 2018) which better reflects human perception. To explicitly demonstrate that GARF is able to infer scenes in the geometry domain, e.g., depth value, we derive depth maps and utilize the metrics Abs Rel, Sq Rel, RMSE and δ in (Wei et al. 2021) to quantitatively evaluate the accuracy of depth maps.
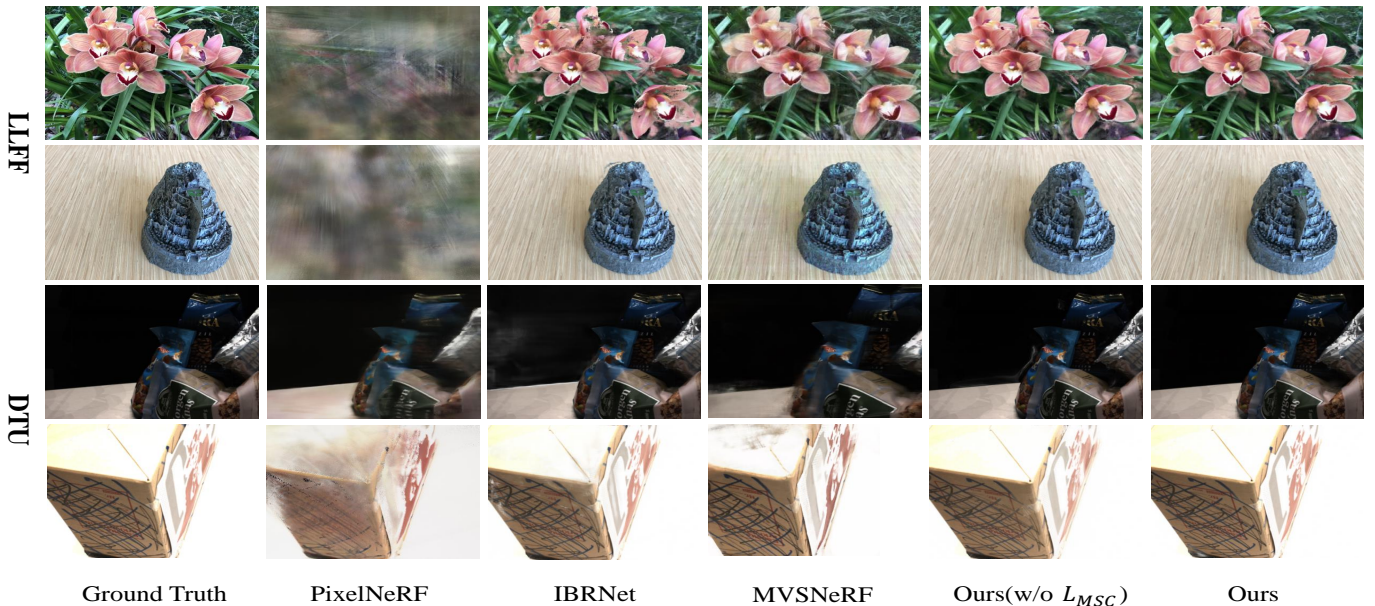
Figure 3: Rendering quality comparison. We show rendering results of our method and concurrent neural rendering methods. The results of PixelNeRF is blurry. IBRNet has some deletions in details and marginal areas. MVSNeRF is not realistic in color and blurred on geometric edges. Our results are more realistic in both geometry-scale and appearance-scale.

Dataset	DTU			LLFF		
Method	PSNR↑	SSIM↑	LPIPS↓	PSNR↑	SSIM↑	LPIPS↓
PixelNeRF	20.62	0.752	0.392	12.31	0.416	0.715
IBRNet	28.71	0.906	0.095	21.68	0.727	0.286
MVSNeRF	26.84	0.946	0.195	21.74	0.764	0.261
Ours(w/o MSC)	34.27	0.983	0.033	22.99	0.775	0.202
Ours	**36.13**	**0.992**	**0.016**	**23.68**	**0.795**	**0.181**

Table 1: Quantitative comparison of rendering. The evaluation metrics are PSNR (higher is better), SSIM (higher is better) and LPIPS (lower is better).

Implementation Details. For the image encoder, we extract features by U-ResNet34. For the sample point feature decoder, we adopt the ray transformer structure with four heads from (Wang et al. 2021). We train every model using the training scenes and test it on unseen test scenes. We use Adam (Kingma and Ba 2017) optimizer with an initial learning rate of 5×10^{-4}, which decays exponentially along with the optimization. We train our network using two RTX 2080 Ti GPUs, spending 30 hours with 128 samples and 10 hours with 40 samples. The values of hyper-parameters mentioned above are set as $\alpha = 1, \beta = 1$.

Results

We compare with the state-of-the-art methods, including PixelNeRF (Yu et al. 2021c), IBRNet (Wang et al. 2021) and MVSNeRF (Chen et al. 2021) in three aspects: 1) The visual quality of the novel-view rendering; 2) the geometry learning ability measured by depth estimation accuracy; and 3) the computational efficiency of each method. All of the results are inferred without per-scene fine tuning.

Novel-view rendering. We qualitatively compare performance of our model with state-of-the-art methods in Fig. 3. We recover fine details more accurately and achieve the most realistic results in both geometry-domain and appearance-

scale. For simple scene like box, we achieve sharper textures, such as the lines on the first row of images. For complicated scene like orchid, prior methods have ambiguity in some positions of the petals, which is probably due to the loss of local information caused by occlusion. Our method fully recovers the geometric structures of scenes, illustrating that by introducing a geometry-aware sampling, GARF is able to better cope with occlusion through geometric priors. More results are provided in supplementary materials.

The quantitative results are shown in Tab. 4. Our model outperforms the other methods on all metrics and datasets. We achieve significant improvement on DTU dataset, outperforming previous works over 20% on PSNR. Our method also realizes 5% improvement on SSIM and 83% improvement on LPIPS. Although the scenes in LLFF are more complicated than DTU and the LLFF dataset is smaller, we still improve 1.94 on PSNR, 4% on SSIM and 31% on LPIPS than the best method before. The results validate that by narrowing down sampling space and using geometry-aware sampling, GARF is excellent in realistic novel-view rendering while preserving generalization to unseen scenes.

Depth Estimation. Rendering quality is closely related to the correct estimation of the scene geometry. GARF has greater awareness of scene geometry, which is proved by its better depth estimation. We show the results in Fig. 4. Even though PixelNeRF has the ability in novel-view rendering, the geometric learning effect of the scene is unsatisfactory. We achieve the best depth estimation which helps improve novel-view rendering, and robustly handle occluded and magnified views. We use the metrics in (Wei et al. 2021; Teed and Deng 2018) to evaluate the accuracy of depth estimation in Tab. 2. The results are tested using the depth ground truth in DTU. We are the best in all met-
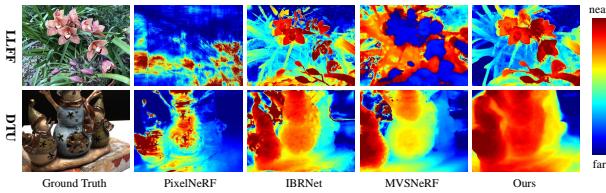
Figure 4: Depth maps derived from four methods on DTU. Our method achieves significantly more accurate depth than the others, illustrating the effectiveness of the geometry-aware sampling strategy. The results also explain the advantage of our method in rendering new perspectives.

Method	Abs Rel↓	Sq Rel↓	RMSE↓	$\delta < 1.25$ ↑	$\delta < 1.25^2$ ↑	$\delta < 1.25^3$ ↑
PixelNeRF	0.3943	0.3127	0.5329	0.3673	0.6212	0.7843
IBRNet	0.0712	0.0108	0.0961	0.9457	0.9965	0.9999
MVSNeRF	0.1698	0.0701	0.2286	0.7584	0.9249	0.9626
Ours	**0.0534**	**0.0099**	**0.0823**	**0.9505**	**0.9986**	**0.9999**

Table 2: Quantitative comparison of the depth estimation on DTU. The metrics are accuracy calculated by l_2 distance.

rics, showing advantage in geometry estimation. Our advantage on depth estimation illustrates that GARF is capable of deriving unseen scenes in geometry-scale, which helps the model perform better in the appearance-scale.

Efficiency. We compare the efficiency of different methods on the number of sampling points in Tab. 3. The number of samples is the sum of sample points in two sampling stages. On DTU dataset, we achieve better PSNR than the state-of-the-art methods when the number of sampling points reduces 25%. On LLFF, we reduce 50% sampling points while achieving 6% improvement on PSNR. Comparing with others, we sample fewer points on the ray, which reduces the time of forward pass, calculation and summation of volume rendering during training and inference. More metrics are provided in the supplementary materials.

Ablation Study

Component Analysis. We first discuss how much our method benefits from the Multi-level Semantic Consistency loss (MSC). To this end, we conduct experiments without MSC while keeping other settings. We present quantitative results in Tab. 4 and visual result in Fig. 3. Though we still achieve better results than the state-of-the-art methods when MSC is removed, the PSNR decreases. In terms of visualization results, the realism of the color and the coherence of the image appearance are decreased, introducing detailed broken textures, especially in areas with thin lines and edges. The utilization of MSC helps the model learn an informative representation and achieve results in high-fidelity.

Then, we verify the validity of GADS strategy. We respectively apply the sampling strategy of NeRF and the GADS to our model on DTU. The results are in Tab. 4. For view synthesis, our sampling strategy has over 6% improvement on PSNR. For depth estimation, our strategy has 11.5% improvement averagely, proving the effectiveness of GADS.

Parameter Analysis. Three important parameters introduced by our method are analyzed in this section. All experiments in this section are performed on LLFF Dataset. The

Dataset	DTU				LLFF			
Method	Samples	PSNR↑	SSIM↑	LPIPS↓	Samples	PSNR↑	SSIM↑	LPIPS↓
PixelNeRF	128 + 64	20.62	0.752	0.392	128 + 64	12.31	0.416	0.715
IBRNet	64 + 64	28.71	0.906	0.095	64 + 64	21.68	0.727	0.286
MVSNet	128	26.84	0.946	0.195	128	21.74	0.764	0.261
Ours	48 + 48	**28.80**	**0.968**	**0.054**	32 + 32	**22.32**	**0.769**	**0.230**

Table 3: Efficiency comparison. We compare the efficiency of different methods by the samples. The number of samples is the sum of sample points in two sampling stages. Our method reduces samples at least 25% with higher PSNR.

Tasks	View Synthesis			Depth Estimation		
Metrics	PSNR↑	SSIM↑	LPIPS↓	Abs Rel↓	Sq Rel↓	RMSE↓
NeRF	33.96	0.979	0.052	0.0682	0.0102	0.0914
Ours	**36.13**	**0.992**	**0.016**	**0.0534**	**0.0099**	**0.0823**

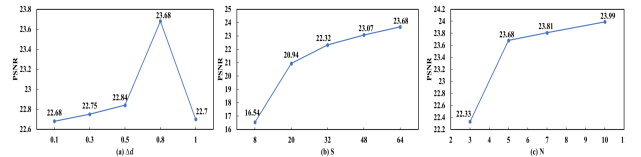Table 4: Ablation study of the sampling strategy.

Figure 5: Results of parameter analysis. We show the change in rendering quality, with the size of the sampling interval, the decrease of samples, and the number of input images.

first is the size of the sampling interval Δd, which is used to control the sampling range. As Fig. 5 (a) shows, we derive the best results at $\Delta d = 0.8$. As Δd decreases, the quality of rendered images decreases, as there is less opportunity to fix depth estimation errors. When the sample interval Δd increases, the awareness of geometry decreases, leading to worse results. The second parameter is the number of sampling points. We show the results in Fig. 5 (b). Before the sampling points drop to 20, image quality is comparable to other methods with 128 sample points, demonstrating the fast rendering capabilities of GARF. But when samples is further reduced, the image quality is noticeably degraded. The reason is that the coarse depth estimation is not very accurate and needs to be further corrected during sampling. The last parameter is the number of input views. The analysis results are shown in Fig. 5 (c). With the increasing of input image number, the quality of the novel view rendering is gradually improved, enabling high quality visual results.

Conclusions

In this paper, we present a geometry-aware generalized neural radiance field GARF with a geometry-aware dynamic sampling (GADS) strategy and a Multi-level Semantic Consistency (MSC) constraint. Extensive experiments have demonstrated that GARF is capable of synthesizing realistic free-viewpoint images and estimating accurate depth map, which proves that GARF preserves the characteristics of each scene while keeping generalization. Besides, the training and inference times of GARF are significantly less than previous generalized NeRFs thanks to its efficient sampling strategy GADS. In the future work, we will explore learning more geometry information to infer accurate geometry surface of scenes and objects.

References

Arandjelovic, R.; and Zisserman, A. 2021. NeRF in detail: Learning to sample for view synthesis. *CoRR*, abs/2106.05264.

Buehler, C.; Bosse, M.; McMillan, L.; Gortler, S.; and Cohen, M. 2001. Unstructured lumigraph rendering. In *Proceedings of the 28th annual conference on Computer graphics and interactive techniques*, 425–432.

Casas, D.; Richardt, C.; Collomosse, J.; Theobalt, C.; and Hilton, A. 2015. 4D Model Flow: Precomputed Appearance Alignment for Real-time 4D Video Interpolation. In *Computer Graphics Forum*, volume 34, 173–182. Wiley Online Library.

Chaurasia, G.; Duchene, S.; Sorkine-Hornung, O.; and Drettakis, G. 2013. Depth synthesis and local warps for plausible image-based navigation. *ACM Transactions on Graphics (TOG)*, 32(3): 1–12.

Chen, A.; Xu, Z.; Zhao, F.; Zhang, X.; Xiang, F.; Yu, J.; and Su, H. 2021. Mvsnerf: Fast generalizable radiance field reconstruction from multi-view stereo. In *Proceedings of the IEEE/CVF International Conference on Computer Vision*, 14124–14133.

Chibane, J.; Bansal, A.; Lazova, V.; and Pons-Moll, G. 2021. Stereo radiance fields (srf): Learning view synthesis for sparse views of novel scenes. In *Proceedings of the IEEE/CVF Conference on Computer Vision and Pattern Recognition*, 7911–7920.

Curless, B.; and Levoy, M. 1996. A Volumetric Method for Building Complex Models from Range Images. In *Proceedings of the 23rd Annual Conference on Computer Graphics and Interactive Techniques*, SIGGRAPH '96, 303–312. New York, NY, USA: Association for Computing Machinery. ISBN 0897917464.

Debevec, P. E.; Taylor, C. J.; and Malik, J. 1996. Modeling and rendering architecture from photographs: A hybrid geometry-and image-based approach. In *Proceedings of the 23rd annual conference on Computer graphics and interactive techniques*, 11–20.

Deng, K.; Liu, A.; Zhu, J.-Y.; and Ramanan, D. 2021. Depth-supervised nerf: Fewer views and faster training for free. *arXiv preprint arXiv:2107.02791*.

Eisemann, M.; De Decker, B.; Magnor, M.; Bekaert, P.; De Aguiar, E.; Ahmed, N.; Theobalt, C.; and Sellent, A. 2008. Floating textures. In *Computer graphics forum*, volume 27, 409–418. Wiley Online Library.

Flynn, J.; Broxton, M.; Debevec, P.; DuVall, M.; Fyffe, G.; Overbeck, R.; Snavely, N.; and Tucker, R. 2019. Deepview: View synthesis with learned gradient descent. In *Proceedings of the IEEE/CVF Conference on Computer Vision and Pattern Recognition*, 2367–2376.

Flynn, J.; Neulander, I.; Philbin, J.; and Snavely, N. 2016. Deepstereo: Learning to predict new views from the world's imagery. In *Proceedings of the IEEE conference on computer vision and pattern recognition*, 5515–5524.

Geyer, C. J. 1992. Practical Markov Chain Monte Carlo. *Statistical Science*, 7(4): 473–483.

Gortler, S. J.; Grzeszczuk, R.; Szeliski, R.; and Cohen, M. F. 1996. The lumigraph. In *Proceedings of the 23rd annual conference on Computer graphics and interactive techniques*, 43–54.

Hedman, P.; Ritschel, T.; Drettakis, G.; and Brostow, G. 2016. Scalable inside-out image-based rendering. *ACM Transactions on Graphics (TOG)*, 35(6): 1–11.

Heigl, B.; Koch, R.; Pollefeys, M.; Denzler, J.; and Gool, L. V. 1999. Plenoptic modeling and rendering from image sequences taken by a hand-held camera. In *Mustererkennung 1999*, 94–101. Springer.

Kingma, D. P.; and Ba, J. 2017. Adam: A Method for Stochastic Optimization. arXiv:1412.6980.

Levoy, M.; and Hanrahan, P. 1996. Light field rendering. In *Proceedings of the 23rd annual conference on Computer graphics and interactive techniques*, 31–42.

Liu, L.; Gu, J.; Zaw Lin, K.; Chua, T.-S.; and Theobalt, C. 2020. Neural Sparse Voxel Fields. In Larochelle, H.; Ranzato, M.; Hadsell, R.; Balcan, M. F.; and Lin, H., eds., *Advances in Neural Information Processing Systems*, volume 33, 15651–15663. Curran Associates, Inc.

Meng, Q.; Chen, A.; Luo, H.; Wu, M.; Su, H.; Xu, L.; He, X.; and Yu, J. 2021. Gnerf: Gan-based neural radiance field without posed camera. In *Proceedings of the IEEE/CVF International Conference on Computer Vision*, 6351–6361.

Mildenhall, B.; Srinivasan, P. P.; Ortiz-Cayon, R.; Kalantari, N. K.; Ramamoorthi, R.; Ng, R.; and Kar, A. 2019. Local light field fusion: Practical view synthesis with prescriptive sampling guidelines. *ACM Transactions on Graphics (TOG)*, 38(4): 1–14.

Mildenhall, B.; Srinivasan, P. P.; Tancik, M.; Barron, J. T.; Ramamoorthi, R.; and Ng, R. 2020. Nerf: Representing scenes as neural radiance fields for view synthesis. In *European conference on computer vision*, 405–421. Springer.

Niemeyer, M.; and Geiger, A. 2021. Giraffe: Representing scenes as compositional generative neural feature fields. In *Proceedings of the IEEE/CVF Conference on Computer Vision and Pattern Recognition*, 11453–11464.

Niemeyer, M.; Mescheder, L.; Oechsle, M.; and Geiger, A. 2020a. Differentiable Volumetric Rendering: Learning Implicit 3D Representations Without 3D Supervision. In *Proceedings of the IEEE/CVF Conference on Computer Vision and Pattern Recognition (CVPR)*.

Niemeyer, M.; Mescheder, L.; Oechsle, M.; and Geiger, A. 2020b. Differentiable Volumetric Rendering: Learning Implicit 3D Representations Without 3D Supervision. In *Proceedings of the IEEE/CVF Conference on Computer Vision and Pattern Recognition (CVPR)*.

Penner, E.; and Zhang, L. 2017. Soft 3D reconstruction for view synthesis. *ACM Transactions on Graphics (TOG)*, 36(6): 1–11.

Teed, Z.; and Deng, J. 2018. Deepv2d: Video to depth with differentiable structure from motion. *arXiv preprint arXiv:1812.04605*.

Trevithick, A.; and Yang, B. 2021. Grf: Learning a general radiance field for 3d representation and rendering. In

Proceedings of the IEEE/CVF International Conference on Computer Vision, 15182–15192.

Wang, Q.; Wang, Z.; Genova, K.; Srinivasan, P. P.; Zhou, H.; Barron, J. T.; Martin-Brualla, R.; Snavely, N.; and Funkhouser, T. 2021. Ibrnet: Learning multi-view image-based rendering. In *Proceedings of the IEEE/CVF Conference on Computer Vision and Pattern Recognition*, 4690–4699.

Wei, Y.; Liu, S.; Rao, Y.; Zhao, W.; Lu, J.; and Zhou, J. 2021. NerfingMVS: Guided Optimization of Neural Radiance Fields for Indoor Multi-View Stereo. In *Proceedings of the IEEE/CVF International Conference on Computer Vision (ICCV)*, 5610–5619.

Yao, Y.; Luo, Z.; Li, S.; Fang, T.; and Quan, L. 2018. MVS-Net: Depth Inference for Unstructured Multi-view Stereo. In *Proceedings of the European Conference on Computer Vision (ECCV)*.

Yu, A.; Fridovich-Keil, S.; Tancik, M.; Chen, Q.; Recht, B.; and Kanazawa, A. 2021a. Plenoxels: Radiance Fields without Neural Networks. *CoRR*, abs/2112.05131.

Yu, A.; Li, R.; Tancik, M.; Li, H.; Ng, R.; and Kanazawa, A. 2021b. PlenOctrees for Real-Time Rendering of Neural Radiance Fields. In *Proceedings of the IEEE/CVF International Conference on Computer Vision (ICCV)*, 5752–5761.

Yu, A.; Ye, V.; Tancik, M.; and Kanazawa, A. 2021c. pixelnerf: Neural radiance fields from one or few images. In *Proceedings of the IEEE/CVF Conference on Computer Vision and Pattern Recognition*, 4578–4587.

Zhang, R.; Isola, P.; Efros, A. A.; Shechtman, E.; and Wang, O. 2018. The Unreasonable Effectiveness of Deep Features as a Perceptual Metric. In *Proceedings of the IEEE Conference on Computer Vision and Pattern Recognition (CVPR)*.